

Constraint percolation on hyperbolic latticesJorge H. Lopez¹ and J. M. Schwarz^{2,3}¹*Department of Civil Engineering, Universidad Mariana, Pasto 520002, Colombia*²*Department of Physics, Syracuse University, Syracuse, New York 13244, USA*³*Syracuse Biomaterials Institute, Syracuse, New York 13244, USA*

(Received 18 December 2015; revised manuscript received 31 May 2017; published 6 November 2017)

Hyperbolic lattices interpolate between finite-dimensional lattices and Bethe lattices, and they are interesting in their own right, with ordinary percolation exhibiting not one but two phase transitions. We study four constraint percolation models— k -core percolation (for $k = 1, 2, 3$) and force-balance percolation—on several tessellations of the hyperbolic plane. By comparing these four different models, our numerical data suggest that all of the k -core models, even for $k = 3$, exhibit behavior similar to ordinary percolation, while the force-balance percolation transition is discontinuous. We also provide proof, for some hyperbolic lattices, of the existence of a critical probability that is less than unity for the force-balance model, so that we can place our interpretation of the numerical data for this model on a more rigorous footing. Finally, we discuss improved numerical methods for determining the two critical probabilities on the hyperbolic lattice for the k -core percolation models.

DOI: [10.1103/PhysRevE.96.052108](https://doi.org/10.1103/PhysRevE.96.052108)**I. INTRODUCTION**

Geometry plays a key role in driving physical processes in such different areas of physics as relativity, cosmology, quantum field theories, and condensed matter [1–7]. In condensed-matter systems, for example, one may consider stochastic processes such as an electron moving through a fixed array of atoms in both Euclidean [8] and hyperbolic geometries [9]. The effect of geometry on the nature of a phase transition is of particular interest [10,11]. For example, hyperbolic spaces possessing a constant negative curvature of -1 have been recently applied to several condensed-matter models, namely the Ising model [12–18] and percolation [19–21].

Why consider hyperbolic spaces? Hyperbolic geometry connects to properties of mean-field theory, as studied on Bethe lattices, with the same nonvanishing surface-to-volume ratio of compact structures as the size of the lattice scales to infinity [16,17]. And yet there are loops at all length scales, as is the case with Euclidean lattices. Accordingly, hyperbolic lattices provide a test bed for studying phase transitions in a geometry that interpolates between Bethe lattices and Euclidean lattices. Hyperbolic lattices are also interesting from a glassy physics perspective because they provide a natural mechanism in two dimensions to frustrate global crystalline order and allow for a more tractable model to study the glass transition and jamming in two dimensions [22,23].

A hyperbolic lattice is a tessellation of the hyperbolic plane, usually denoted by the so called Schläfli symbol $\{P, Q\}$, where regular polygons of P sides tile the plane so that Q of these polygons meet at each vertex [24], and P, Q satisfy the relation

$$(P - 2)(Q - 2) > 4. \quad (1)$$

It should be noted that (i) Euclidean lattices satisfy the equation $(P - 2)(Q - 2) = 4$, and (ii) for lattices on the elliptic plane, the relation $(P - 2)(Q - 2) < 4$ holds [25]. Therefore, the elliptic and Euclidean planes admit just a finite number of tessellations, while the hyperbolic plane is much richer, admitting an infinite number. We will use the Poincaré disk representation of the hyperbolic plane, which is the unit radius disk with its respective metric [26].

We will work with several hyperbolic tessellations, an example of which is seen in Fig. 1, to study k -core [27,28] and force-balance [29] percolation models and explore the nature of their transition. Both models are examples of constraint percolation in that they go beyond the usual random dilution of sites on a lattice, otherwise known as percolation. There are constraints on the dilution (or occupation) of sites. k -core percolation is a constraint percolation model in which occupied sites having less than k occupied neighboring sites are pruned starting with an initial random and independent occupation of sites. This pruning is done consecutively until all occupied sites have at least k occupied neighboring sites. This constraint imposes the scalar aspect of the local Hilbert stability criterion for purely repulsive particles, i.e., $k \geq d + 1$ in d dimensions [30], and therefore it may explain how purely repulsive particles form a jammed packing [28].

In mean field, k -core percolation resembles some properties of a mixed phase transition [28], i.e., discontinuity in the order parameter and a diverging length scale, as in the jamming transition [31]. And yet, k -core percolation on Euclidean lattices appears to exhibit either a continuous phase transition in the same universality class as ordinary percolation [32], or no transition [33]. So we ask the following questions: What is the nature of the k -core percolation transition on hyperbolic lattices? Will the transition behave more like what is found on the Bethe lattice?

To enforce the local Hilbert stability condition beyond just the scalar aspect in two dimensions, at least three neighboring particles must enclose a particle within a triangle so that forces balance and each particle is locally mechanically stable. This condition has been encoded in a constraint percolation model known as force-balance percolation [29]. Accordingly, the force-balance model introduces the notion of force stability, which is not taken into account by the k -core models. Such a constraint does not allow for finite clusters, at least in Euclidean geometries, which is very different from k -core percolation. The force balance model was studied in two and three dimensions [29]. Numerical simulations suggested strong signs of a discontinuous transition in the standard order parameter (i.e., the fraction of sites participating in the

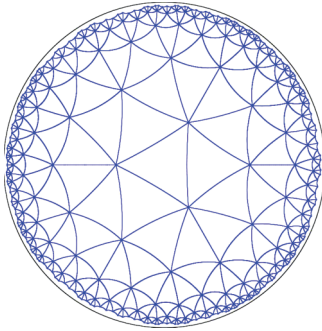


FIG. 1. {3,7} tessellation on the Poincaré disk.

spanning cluster), which also occurs in jamming. Numerical simulations also suggested that there exists a correlation length scale diverging faster than any power law; this is different from jamming, where numerics suggests a more standard power-law diverging correlation length [34]. We expect force-balance percolation to exhibit a discontinuous percolation transition on hyperbolic lattices since it already appears to be in the presence of many loops [28,29]. Perhaps, however, the diverging length scale on the hyperbolic lattice will be a power law, as opposed to faster than a power law on the Euclidean lattice. In any event, the discontinuity in the onset of the spanning cluster should give us something to compare against when trying to determine whether or not k -core percolation exhibits a discontinuous transition on hyperbolic lattices.

As you will soon discover, many of the numerical techniques developed for the analysis of the phase transition in ordinary percolation are not as readily applicable on hyperbolic lattices given the strong boundary effects, which makes the above questions slightly difficult to answer. There also exists the possible complication that there are two phase transitions, as has been demonstrated for ordinary percolation—one transition at the onset of many spanning clusters touching the boundary, and a second transition at the onset of all of the spanning merging into just one spanning cluster [21]. Reference [35] asked the above questions for the $k = 3$ case and concluded, based on a conjecture and on numerical evidence, that the mixed nature of the $k = 3$ -core percolation transition on the Bethe lattice was robust on the hyperbolic lattice. In light of more recent work identifying crossing probabilities on the hyperbolic lattice for ordinary percolation [18], we revisit the above questions for $k = 3$ -core percolation and analyze the other k -core models as well as force-balance percolation.

The remainder of this paper is organized as follows: We will study several properties of k -core percolation models for $k = 1, 2, 3$, and force-balance percolation on hyperbolic tessellations. We present in Sec. II details of the hyperbolic lattice and various percolation algorithms. In Sec. III, we present theoretical proof that the threshold for force-balance percolation is strictly less than 1 for most of the tessellations. This section is a bit technical, and it can be skipped if the reader is more interested in the nature of the phase transition. We present our numerical results in Sec. IV, where we study the crossing probability and other measurements. We summarize and discuss the implications of our results in Sec. V.

II. MODEL AND METHODS

The key step in the simulation process is to construct a hyperbolic lattice. We do this by implementing the algorithm described in detail in Ref. [36]. In the construction of a $\{P, Q\}$ hyperbolic lattice, where again P denotes the number of sides of each polygon and Q denotes how many polygons meet at a vertex, the central polygon is built first, and this is the first layer. Then, by translations and rotations of the central polygon, the second layer is built. This process is followed recursively until a desired number of layers is constructed. An l layer is composed of those polygons that do not belong to an m layer for $m < l$ and share an edge or vertex with a polygon in the $(l - 1)$ layer. The algorithm makes use of the *Wierstrass model* for hyperbolic geometry, where points lie on the upper sheet of the hyperboloid, $x^2 + y^2 - z^2 = -1$. Consequently, rotations and translations are given by 3×3 Lorentz matrices. The Wierstrass model is related to the Poincaré model through the stereographic projection toward the point $(0, 0, -1)^t$ given by

$$\begin{pmatrix} x \\ y \\ z \end{pmatrix} \rightarrow \frac{1}{1+z} \begin{pmatrix} x \\ y \\ 0 \end{pmatrix}. \tag{2}$$

The exponential growth of the number of vertices with respect to the number of layers constrains severely the number of layers used in the simulations. Typically, we simulate around 10 layers. This is comparable to the recent work by Gu and Ziff studying ordinary percolation on hyperbolic lattices [18]. Recent work on implementing periodic boundary conditions in certain tilings may ultimately be investigated [37]. However, the sets of hyperbolic tilings that can be used with the methods in Ref. [37] have fewer than 30 000 sites due to a lack of knowledge of all possible normal subgroups of a given Fuchsian group.

Once a tessellation is created, each of its sites is occupied with probability p . For k -core percolation, we then recursively remove any occupied site (excluding boundary sites) that has fewer than k occupied neighboring sites. For force-balance percolation, we recursively remove any occupied sites (excluding boundary sites) that are not enclosed by a triangle of neighboring occupied sites, i.e., those sites that are not locally mechanically stable. We do this until all occupied sites obey the imposed constraint. We have numerically tested about one million runs, so that the order in which we check the force-balance constraint does not affect the final configuration, i.e., that the model is Abelian. It has also been argued that the k -core model is Abelian [38].

We then use the Hoshen-Kopelman algorithm to identify the clusters and their respective sizes. To determine if a cluster is spanning, we break up the lattice into four cardinal regions: NE, NW, SW, and SE. See Fig. 2. We regard the cluster as percolating, or spanning, when it connects either NE and SW sites or NW and SE sites, as in Ref. [18]. We then measure the probability to span or cross for an occupation probability p , and we denote it $R(p)$. We also measure a quantity defined as S_1/N , where S_1 is the size of the largest cluster and N is the total number of sites. This quantity resembles the order parameter and, therefore, determines the continuity or discontinuity of the onset of the transition(s), i.e., should it

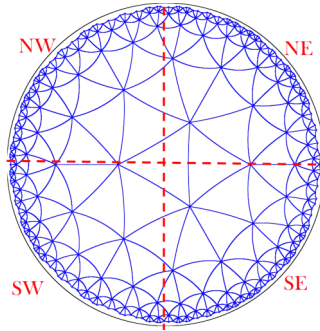


FIG. 2. {3,7} tessellation on the Poincaré disk with the four boundary regions.

increase from zero continuously as the occupation probability p is increased, then the transition is continuous. We also measure the number of times we check the lattice to cull occupied sites not obeying their respective constraints, i.e., the culling time. This *culling time* tends to diverge near the transition on Euclidean lattices [29].

III. PROOF OF $p_{FB} < 1$ FOR SOME HYPERBOLIC TILINGS

It has been established that there exist two critical percolation probabilities, p_l and p_u , for ordinary percolation on hyperbolic tilings [20,39,40]. For the force-balance model, however, it seems that there is just one critical percolation probability, according to the results presented later, demonstrating the emergence of a percolating cluster. Let us call this probability, p_{FB} , the probability above which there is always a percolating cluster. It is possible to prove that $p_{FB} < 1$ for some hyperbolic tilings $\{P, Q\}$. The proof follows two steps:

(i) First establish the existence of trees on a tessellation $\{P, Q\}$ with a certain connectivity that depends on the parity of Q . For Q even we demand a connectivity $z = 6$, and for Q odd, $z = 5$.

(ii) We apply a well-known result of k -core percolation on trees, i.e., that the critical percolation is less than 1 when $k < z$ [27]. For our purposes, we require $k = 5$ for tessellations of Q even and $k = 4$ for Q odd. Accordingly, we show that sites on a percolating cluster for the $k = 5$ -core model on the $z = 6$ trees, and Q even, satisfy the occupation constraints of the force-balance percolation model. Similarly, for the Q -odd case, we study the $k = 4$ -core model on $z = 5$ trees.

Let us prove each of these items in due order. First, we need to show the existence of trees of connectivity $z = 6$ and 5 for Q even and odd, respectively. Let us suppose Q is even. It is easy to see that $z = 6$ trees cannot be built when $Q = 4, 6$ as there is not enough “space” to build trees given the eventual overlaps. The case $Q = 8$ is more interesting. The tessellation $\{3, 8\}$ does not admit a tree construction due to overlaps, as illustrated in Fig. 3, where red arrows show some of those positions at which the initial tree (green) eventually contains overlaps. However, $z = 6$ trees can be built on the tessellation $\{4, 8\}$. To see this, we choose a site that we call the zeroth generation. The first generation are the neighbors of such a site. The n th generation will be formed by those site neighbors of the $(n - 1)$ th generation that do not belong to a k th generation

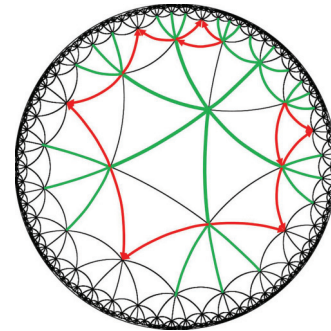


FIG. 3. One cannot embed a tree of connectivity $z = 6$ on the $\{3, 8\}$ tessellation due to the lack connections.

where $k < n$. This is illustrated in Fig. 4. By construction, between two adjacent first-generation sites on the $z = 6$ tree there is one second-generation site that does not belong to the tree. Now between the closest offspring of those first-generation sites that are second-generation sites belonging to the tree, there are six third-generation sites not belonging to the tree. By construction, such trees can be expanded without overlapping so that they, indeed, remain trees.

For $P > 4$ we have more vertices in each layer, which gives more space to build trees, and the same construction holds. Accordingly, we can build $z = 6$ trees on the tessellation $\{P, 8\}$ when $P > 3$. Likewise, it can be checked that for any P, Q even, and $Q > 9$, it is possible to build a tree of connectivity $z = 6$. Analogously, trees of connectivity $z = 5$ can be built on tessellations $\{P, 7\}$ where $P > 3$, and for any tessellation $\{P, Q\}$ where $Q > 8$ is odd.

In summary, those trees necessary for our proof can be built on any tessellation $\{P, Q\}$ as long as $Q > 8$ and for the tessellations $\{P, 7\}, \{P, 8\}$ as long as $P > 3$.

As for the second step in the proof, consider any site on the tree built in step (i). A site of a $\{P, Q\}$ tessellation will be contained in a Q -gon as illustrated in Fig. 5. Now let us take such Q -gons in a Euclidean setting as illustrated in Fig. 6. One of the neighbors of the central site is isolated from the others. Let us call it the north neighbor, NN. It happens that any tree of connectivity $z = 4$ (Q even case) containing site NN and imbedded in those trees of connectivity $z = 5$ satisfies the force-balance constraint as indicated in Fig. 7. In two dimensions, this constraint is that every occupied site

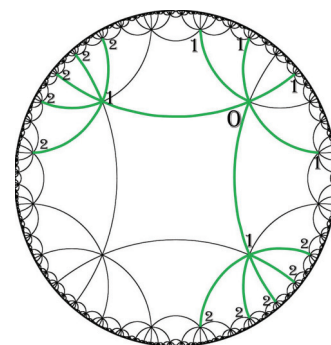


FIG. 4. Tessellation $\{4, 8\}$ enables the construction of trees of connectivity $z = 6$.

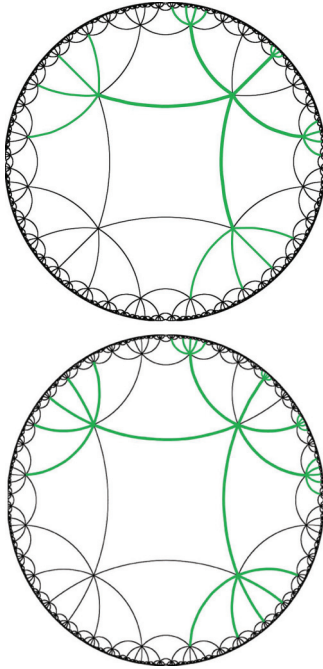


FIG. 5. Tree construction on tessellations {4,7} and {4,8}: Top: tree of connectivity $z = 5$ on the {4,7} tessellation. Bottom: tree of connectivity $z = 6$ on the {4,8} tessellation.

(particle) have at least three neighboring occupied sites, and at least three of these neighboring sites enclose the occupied site in a triangle. This *triangle* condition on the central site is preserved in the hyperbolic geometry given that the function that relates those polygons in different geometries preserves topology. A similar proof applies to trees of connectivity $z = 5$ embedded in trees of connectivity $z = 6$ (Q -even case).

The above analysis holds for any site, so we can always construct such a Q -gon with the same characteristics for any occupied site. Now let us call p_{4c} the critical percolation probability for $k = 4$ -core percolation on trees of connectivity $z = 5$, and p_{5c} is such probability for $k = 5$ -core percolation on trees of connectivity $z = 6$. It follows from the discussion above that $p_{FB} < p_{4c}$ for Q even, and $p_{FB} < p_{5c}$ when Q is odd (search p_{4c} and p_{5c}), at least for those tessellations where we can make the tree construction illustrated in Fig. 5. Since both p_{4c} and p_{5c} are less than unity for the trees enumerated, $p_{FB} < 1$.

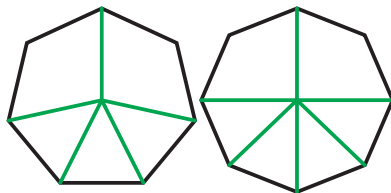


FIG. 6. Euclidean illustration of the central part of the trees on hyperbolic tessellations: Left: Euclidean illustration of the “central” part of the $z = 5$ tree on tessellation {4,7}. Right: Euclidean illustration of the “central” part of the $z = 6$ tree on tessellation {4,8}.

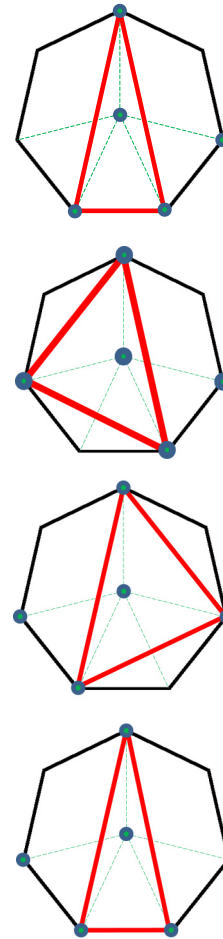


FIG. 7. Illustration of all the possible cases of occupation for a $k = 4$ -core cluster on a tree of connectivity $z = 5$.

IV. RESULTS

We work with tessellations {3,7}, {7,3}, and {4,7}, where the first two tessellations are the most commonly studied [18,20]. We study $k = 1, 2, 3$ -core percolation and force-balance percolation on such tessellations by computing the crossing probability, R , the probability of participating in the largest cluster, P_{LC} , and the culling time.

A. Crossing probability

Ordinary percolation exhibits three phases on the hyperbolic lattice [21]. Specifically, for $p < p_l$ there is no percolating cluster, for $p_l < p < p_u$ there are infinitely many percolating clusters, and for $p > p_u$ the infinitely many percolating clusters merge to form just one percolating cluster. The existence of three phases is reflected in the crossing probability, $R(p)$. According to Ref. [18], as the number of layers tends to infinity, $R(p)$ tends to a function that in the intermediate phase is a straight line with finite slope in the infinite layer limit. If there is just one phase boundary, as with ordinary percolation on Euclidean lattices, then in the infinite system limit $R(p)$ jumps discontinuously at the boundary from 0 to 1 through some value of $R(p_c)$, the Cardy crossing value [41], at the transition. So there would be no finite slope region in the infinite system limit.

Since $k = 1$ -core percolation removes only isolated occupied sites, it is essentially ordinary percolation. We should therefore observe this finite slope intermediate region in the crossing probability as the number of layers tends toward infinity. This finite slope region has indeed been observed in Ref. [18] for $k = 0$ -core, or ordinary, percolation. Figure 8 presents the crossing probability for all four percolation models. To check for the existence of the intermediate region in $R(p)$, we extract its maximum slope M_0 near the inflection point. We then plot the inverse of this slope as a function of the $1/\ell$ and extrapolate to the number of layers, ℓ , going to infinity limit. The results are illustrated in Fig. 9. The inverse of the slope, $1/M_0$, tends to similar values for $k = 1$ -core and $k = 2$ -core models. For $k = 1$ core it tends to 0.240 ± 0.004 , and 0.223 ± 0.010 for the $k = 2$ -core model. Meanwhile, $1/M_0$ tends to 0.131 ± 0.007 for the $k = 3$ -core model.

The fact that the inverse of the slope tends to -0.016 ± 0.020 for the force-balance model, which is zero within a standard deviation of the intercept when making the respective linear regression, is an indication that the slope tends to infinity at the transition. Then the force-balance model would exhibit just two phases, one with no percolating cluster and the other with one percolating cluster as ordinary percolation on Euclidean lattices. To make a more rigorous case for the discontinuity of the crossing probability for the force-balance model, we analyze the tendency of the inverse of the slope $1/M_0$ against $1/\ell$ for points located on the intersection with the lines $R(p) = c, c \in \mathbb{R}$. For $c = 0.3, 0.4, 0.5, 0.6, 0.7$, the inverse of the slope tends to a value that is close to zero but negative. This confirms the argument that $R(p)$ is discontinuous for the force-balance model, and, consequently, there should be just two phases for this model.

The suggestion of a finite slope regime of $R(p)$ for all three k -core percolation models suggests that there is an intermediate phase for all these models. In other words, all three models behave similarly to ordinary percolation. Of course, we have empirically chosen a function to implement the extrapolation. In Ref. [18], the maximum slope M as a function of $N^{-0.7}$, where N is the number of vertices in the tessellation, was used. We also tested slightly different extrapolation functions, and our results remain unchanged in terms of the interpretation.

B. Order parameter

For ordinary percolation on Euclidean lattices, the order parameter P_∞ is a continuous function of p [42]. Since the $k = 1$ - and $k = 2$ -core models are equivalent to unconstrained percolation in terms of the transition, they should behave similarly. While the order parameter in $k = 3$ core on the Bethe lattice jumps discontinuously at the transition [27], on Euclidean lattices it does not. For force-balance percolation on two- and three-dimensional Euclidean lattices, the order parameter jumps discontinuously at the transition [29]. We present $P_\infty(p)$ for different layer numbers for the four different models on the $\{3, 7\}$ tessellation in Fig. 10. Since any difference between the curves is not clear by eye, we perform a similar extrapolation to what was used for the study of $R(p)$. We measure the maximum slope of each curve and plot the inverse of the maximum slope, $1/S_0$, with respect to $1/l$. We found

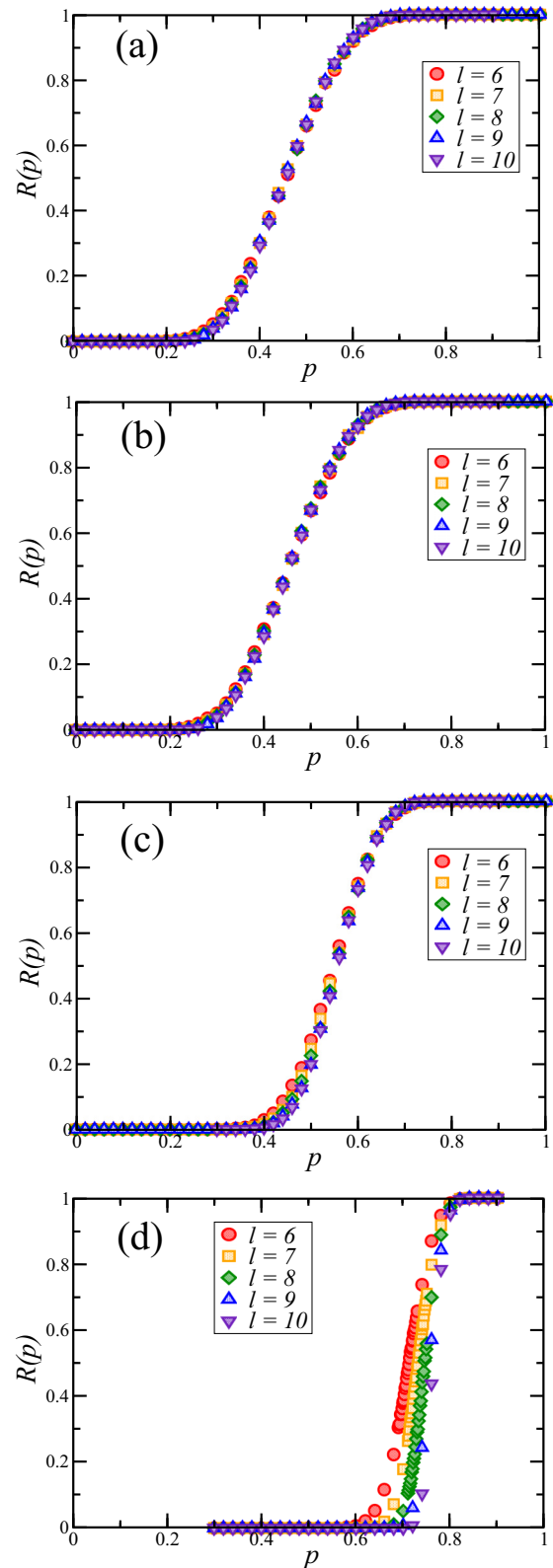


FIG. 8. Crossing probability on $\{3, 7\}$ tessellation for the different percolation models: (a) $k = 1$ core, (b) $k = 2$ core, (c) $k = 3$ core, and (d) force balance.

that the k -core models have very similar values for $1/S_0$ when l tends to infinity, i.e., 0.113 ± 0.002 , 0.120 ± 0.003 , and 0.111 ± 0.002 for the 1-core, 2-core, and 3-core models,

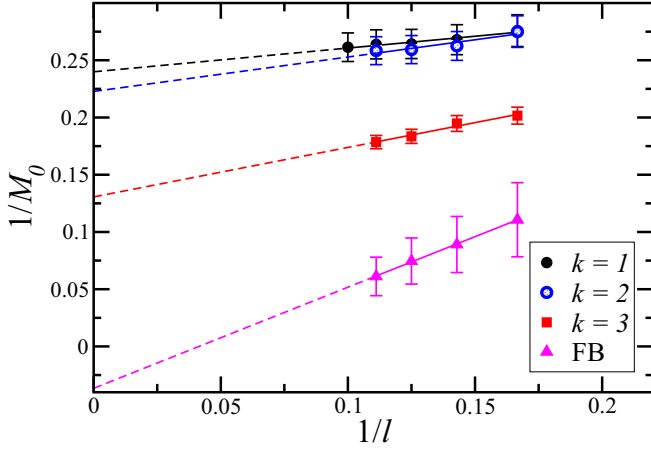


FIG. 9. Inverse slope of the crossing probability at the inflection point, $1/M_0$, as a function of $1/l$ for the different percolation models on the $\{3,7\}$ lattice. For the 1-core model, $1/M_0$ tends to 0.240 ± 0.004 ; for 2-core, to 0.223 ± 0.010 ; for 3-core, to 0.131 ± 0.007 ; and for force-balance (FB), to -0.016 ± 0.02 , indicating M_0 is tending to ∞ as l tends to ∞ .

respectively (see Fig. 11). The k -core models may indeed be continuous phase transitions for the $\{3,7\}$ tessellation. For the force-balance model, the same extrapolation method yields a negative value, as shown in Fig. 11, but one that is close to zero. In other words, the negative sign is due to the errors in the measurement of $1/S_0$. This result may indicate that force-balance percolation belongs to a discontinuous phase transition. This result is expected since it is discontinuous on Euclidean lattices as well. To make a clearer statement about the discontinuity of the force-balance transition, we analyze the behavior of the derivative for points on a line $P_\infty = c, c \in (0, 1)$. We present the extrapolation of the inverse of this derivative $1/S$ versus the inverse number of layers $1/l$ for the values $c = 0.3, 0.4, 0.5, 0.6, 0.7$ in Fig. 12. We conclude that as $1/S$ is tending to zero for several values of the constant c , then P_∞ is discontinuous, implying that the force-balance model is discontinuous on the tessellation $\{3,7\}$.

Note that it is interesting that the 3-core model is exhibiting a continuous transition given that Sausset *et al.* [35] argue that the transition should be discontinuous. However, they do not study the tessellation $\{3,7\}$, and the criterion they used for a percolating cluster contains the central site and reaching the boundary, which is different from the criterion we use as we require the percolating cluster to connect the two opposite boundary quarter sites. To better connect with this prior work, we also study the case for which we require the central site to be occupied when determining the percolating cluster. Our results with this added constraint reach the same conclusion as before, i.e., a continuous transition, with $1/S_0 = 0.112 \pm 0.007$. We should note that Sausset *et al.* [35] did not employ any extrapolation method to more carefully check for the nature of the transition with regard to the order parameter, as we have done.

C. Culling time

The culling time is the number of sweeps through the lattice to complete the culling and removal process for those occupied

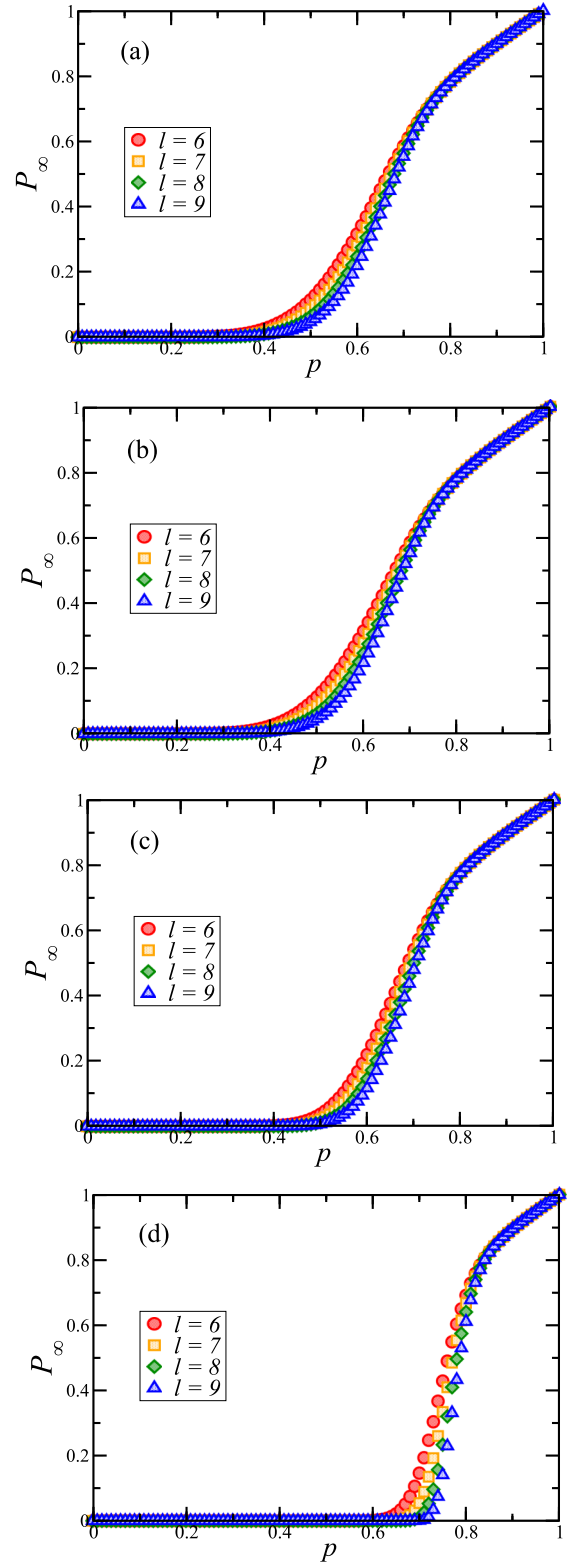


FIG. 10. The fractional size of the largest cluster P_{lc} for the different percolation models on the $\{3,7\}$ lattice: (a) $k = 1$ core, (b) $k = 2$ core, (c) $k = 3$ core, and (d) force balance.

sites not obeying the respective constraints. On Euclidean lattices, the culling time for $k = 3$ core and force-balance percolation increases near the percolation transition due to an increasing length scale in the distance over which the removal

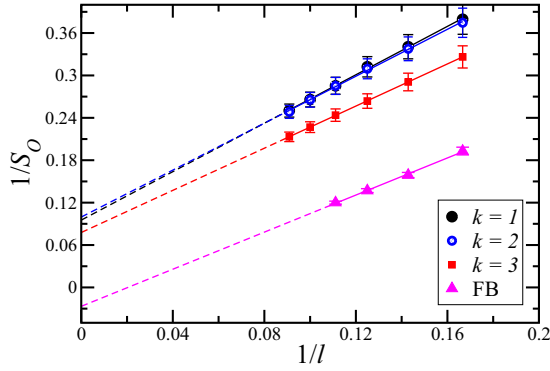


FIG. 11. The inverse of the maximum slope of P_∞ as a function of l for the different models' percolation on the $\{3,7\}$ lattice.

of one occupied site triggers the removal of other occupied sites.

In Fig. 13, we observe the culling time for tessellation $\{3,7\}$, for $k = 2,3$ core and force-balance models. Note that for $k = 1$ core it just takes one sweep of the lattice to eliminate sites not satisfying the constraint, so there is no diverging length scale. According to Fig. 13, there is a peak in the culling time T as a function of p . Note that the position of the peak for the k -core models does not move as the number of layers increases. However, for the force-balance model the peak is increasing with the number of layers. We obtain the extrapolated $p_{FB}^* \approx 0.837$ when scaling p_{FB} as l^{-1} . We approximate each curve to a Gaussian function $f(x) = Ae^{-(x-x_0)^2/2\sigma^2}$ in a region close to the peak. The tendency of σ versus $1/l$ is illustrated in Fig. 14. Therefore, the width σ tends to a finite value for the k -core models, 0.196 for 2-core and 0.210 for 3-core, while it shrinks to zero for the force-balance model. Furthermore, the height of the peak tends to infinity for all these peaks. A peak that remains broad in the infinite system limit may be indicative of the two percolation thresholds in the ordinary percolation model that appear to survive in the $k = 2$ - and $k = 3$ -core models.

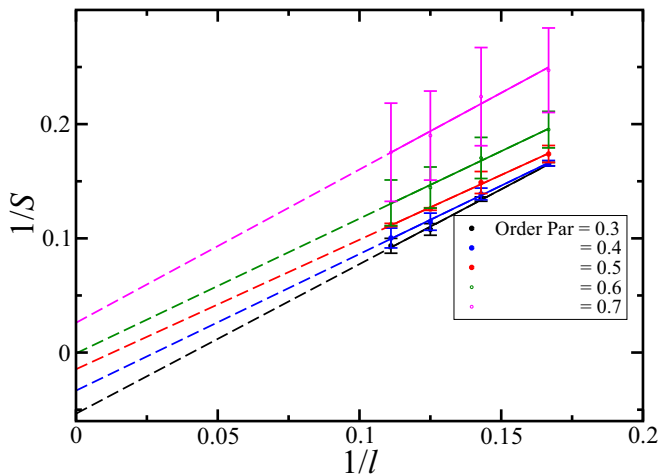


FIG. 12. Inverse slope of P_∞ , $1/S$, tendency on $1/l$ for points on the line $P_\infty = c$ and $c = 0.3, 0.4, 0.5, 0.6, 0.7$, for the force-balance model on the $\{3,7\}$ lattice.

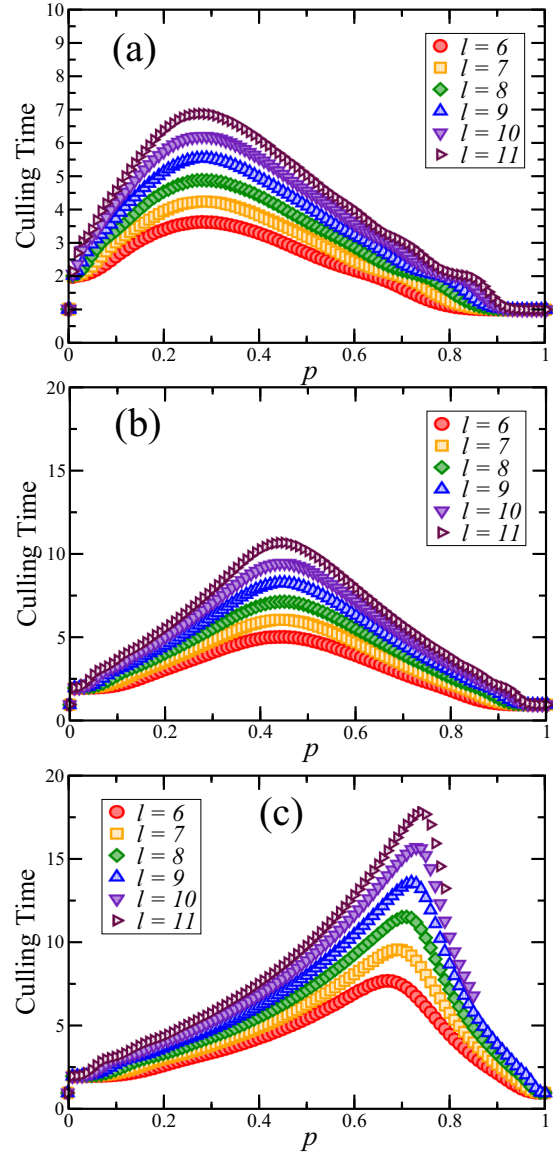


FIG. 13. Culling time for the different constraint percolation models for the $\{3,7\}$ lattice: (a) $k = 2$ core, (b) $k = 3$ core, and (c) force balance. Each data set was averaged over 50 000 samples.

D. Debate about p_u

There exist three phases for ordinary percolation on a hyperbolic lattice [21]. For $p < p_l$ there is no percolating cluster, for $p_l < p < p_u$ there are infinitely many percolating clusters, and for $p_u < p$ the infinite number of percolating clusters join, forming one. There is no clear consensus, however, about how to numerically calculate p_l and p_u [43]. According to Ref. [20], p_l can be measured as the probability above which there is a cluster connecting boundary points to the center. But p_u can be measured in three different ways. The probability above which the ratio between the second biggest cluster and the biggest cluster, S_2/S_1 , becomes negligible, or there is a finite fraction of the boundary points connected to the middle, or the probability at which the cluster size distribution $P(s)$ becomes power law. Furthermore, for calculating p_u , Ref. [20] determines a way of finding p_u by measuring the

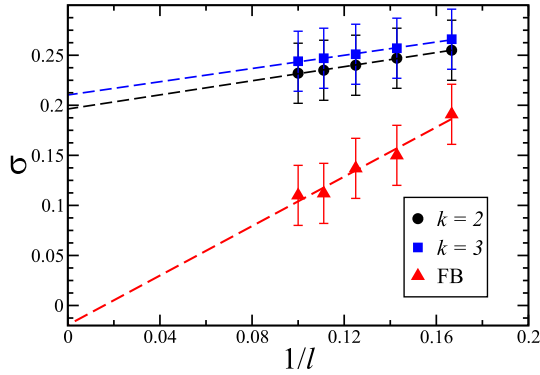


FIG. 14. Behavior of the width σ vs $1/l$ for the 2-core, 3-core, and force balance models on the $\{3,7\}$ lattice.

ratio S_2/S_1 between the second largest and largest clusters. The initial claim was that in the infinite limit such a curve will be discontinuous at some intersection point (see their Fig. 4). However, in a more recent paper [43], the same authors stated that it could be the case that the curve is not discontinuous at this point, such as the curves for $R(p)$. In fact, according to Fig. 15 this seems to be the case here for the $k = 1$ -core model (and for the other two k -core models as well). So we do not rely on this method any further.

According to Ref. [18], p_l and p_u can be measured from the crossing probability $R(p)$, i.e., the probability of having a cluster going from one side of the lattice to the other. While this is the more straightforward measure, it would be good to find other measurements as a consistency check. It is important to note that there is a relationship between p_l and p_u on a lattice and its values on the dual lattice that are denoted as \bar{p}_l and \bar{p}_u , respectively. Such a relationship is given by [40]

$$p_l + \bar{p}_u = 1, \quad \bar{p}_l + p_u = 1, \quad (3)$$

and the dual lattice to $\{m, n\}$ is $\{n, m\}$ [18]. As the measurement of p_l is less controversial than the one for p_u , we can use Eq. (3) to calculate p_u by calculating \bar{p}_l on the dual lattice. To estimate p_l , we search for the point at which the crossing probability is greater than or equal to 10^{-4} , similar to the procedure followed in Ref. [18]. For these calculations, the data were averaged over 100 000 runs and have large fluctuations. We estimate p_l for the k -core models on the tessellation $\{3,7\}$. For $k =$

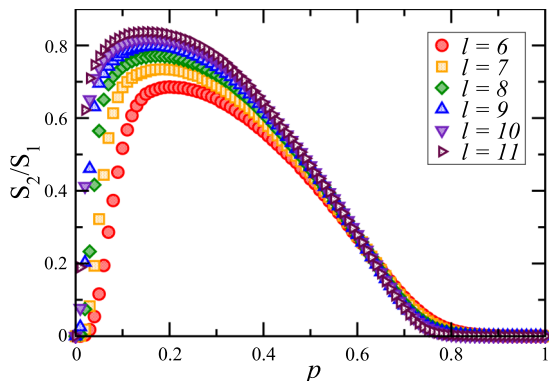


FIG. 15. Ratio S_2/S_1 for $k = 1$ core and for the tessellation $\{3,7\}$.

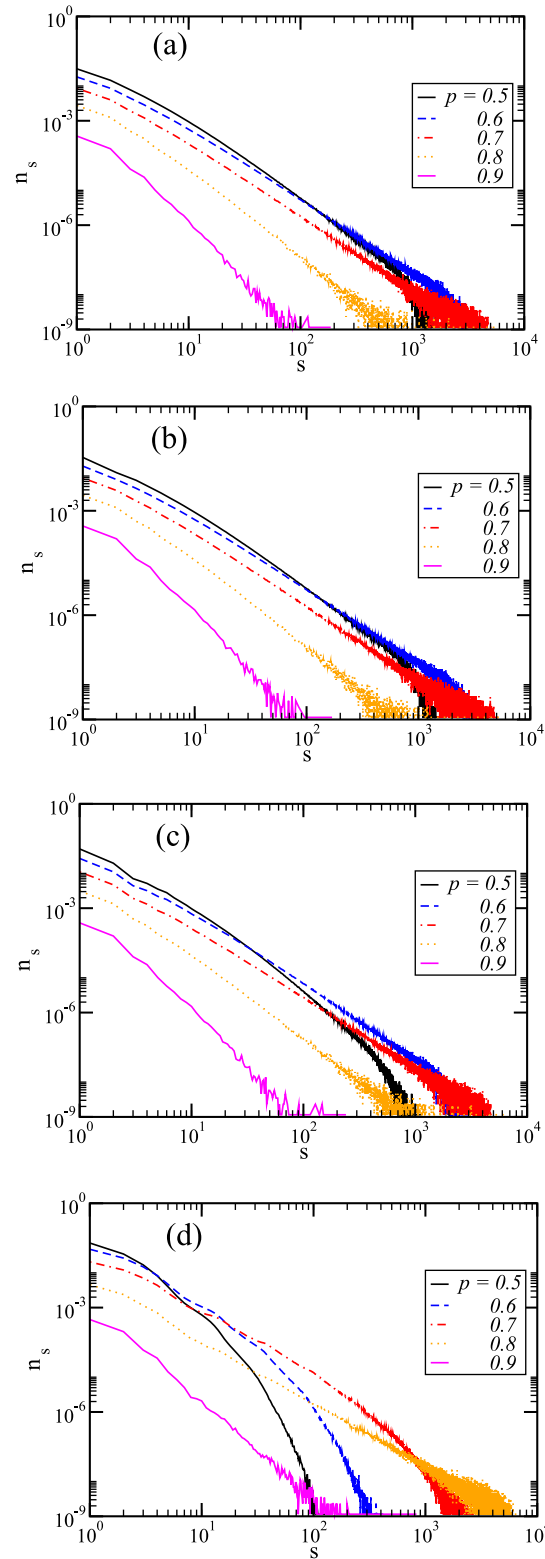


FIG. 16. Cluster size distribution n_s for the different percolation models in the $\{3,7\}$ lattice: (a) $k = 1$ core, (b) $k = 2$ core, (c) $k = 3$ core, and (d) force balance.

1-core, $p_l = 0.20$; for $k = 2$ -core, $p_l = 0.24$; and for $k = 3$ -core, $p_l = 0.37$. According to Eq. (3), for ordinary percolation ($k = 1$ -core) on tessellation $\{7,3\}$, we should have $p_u = 0.80$. To estimate p_u numerically (for the $k = 1$ -core model), we

follow the procedure outlined in Ref. [18] stating that p_u is the value of p at which the ratio of the crossing probability $R(p)$ becomes equal to 1 for tessellations $\{3,7\}$ and $\{7,3\}$. Accordingly, the best estimate for p_u for the tessellation $\{3,7\}$ is $p_u = 0.73 \pm 0.02$, and for the tessellation $\{7,3\}$ it is $p_u = 0.86 \pm 0.02$, which roughly satisfies Eq. (3).

E. Cluster size distribution

Finally, we study the number of clusters of a given size s normalized by the number of lattice sites, n_s , for a given p on tessellation $\{3,7\}$ with nine layers. The spanning cluster is not taken into account when computing n_s . The results for each model are presented in Fig. 16. It was illustrated in Ref. [20] that the probability of finding a cluster with a given size s , for ordinary percolation, shifts from a truncated power law to a power-law distribution when p passes the upper critical probability p_u . However, Ref. [20] did not register any change in the qualitative behavior of the distribution when probability p passed the lower critical probability p_l . We see the same qualitative behavior for all the models studied. According to the cluster size distribution for the three k -core models, all have a similar value for p_u that is somewhat close to $p = 0.7$ since n_s is broadest at that occupation probability. Interestingly, the cluster size distribution for the force balance model exhibits similar characteristics to those of the k -core models.

V. DISCUSSION

We have studied four constraint percolation models on mainly the $\{3,7\}$ hyperbolic tessellation. Our data suggest that all three k -core models exhibit similar behavior, thereby falling under the universality class of ordinary percolation. This is not a surprise for $k = 2$ -core percolation, which has been shown to behave similarly to ordinary percolation [44]. However, given the mixed $k = 3$ -core percolation transition on Bethe lattices and, yet, the continuous phase transition (should $p_c < 1$) on Euclidean lattices for $k = 3$ -core, this result is not obvious. In fact, earlier work [35] of $k = 3$ -core percolation on hyperbolic lattices argued that the transition behaves discontinuously based on arguments and when looking at numerical data for the onset of the order parameter. We have employed a

more detailed numerical analysis here suggesting a continuous transition, which does not contradict mathematics at this point since no proof of a discontinuity has yet to be put forth. So while our data suggest that all three k -core models exhibit a continuous transition, the transition for force-balance percolation is discontinuous, at least on the $\{3,7\}$ tessellation. Force-balance percolation is also discontinuous on Euclidean lattices, so the hyperbolic lattice does not change this property by the changing of the underlying geometry. The severity of the constraints (more severe than k -core) presumably result in the model being less sensitive to the geometry. We also have presented proof that $p_{FC} < 1$ for some tessellations, which can be very useful in constraining the interpretation of the data.

Another interesting result is that the k -core models exhibit two critical probabilities, p_l and p_u , while the force-balance model seems to exhibit just one critical probability. This comes from the fact that the force-balance condition constrains the spatial occupation of neighbors of an occupied site in such a way that the cluster tends to expand in every direction. It does not allow for the possibility of having several percolating clusters that do not overlap.

The observation that the nature of the transition in $k = 3$ -core percolation does not change from Euclidean lattices to hyperbolic lattices may indicate that (the absence of) loops are important in driving the transition toward a mixed one since on the Bethe lattice there are no loops. In other words, $k = 3$ -core percolation may be very sensitive to loops. A $1/d$ expansion for $k = 3$ -core percolation demonstrated that the mixed nature of the transition remained to order $1/d^3$ [45]. Of course, the loops are controlled perturbatively in this $1/d$ expansion, which is not the case for the hyperbolic tessellation. One must think about the effects of loops on $k = 3$ -core percolation to better understand the nature of its transition in all geometries.

ACKNOWLEDGMENTS

J.M.S. acknowledges support from NSF-DMR-CMMT-1507938 and the Soft Matter Program at Syracuse University. J.H.L. acknowledges financial support from the Centro de Investigaciones CEI, Universidad Mariana.

-
- [1] S. Carroll, *Spacetime and Geometry: An Introduction to General Relativity* (Addison-Wesley, Reading, MA, 2003).
 - [2] P. Fleury, H. Dupuy, and J.-P. Uzan, Can all Cosmological Observations be Accurately Interpreted with a Unique Geometry, *Phys. Rev. Lett.* **111**, 091302 (2013).
 - [3] M. D. Maia, *Geometry of the Fundamental Interactions: On Riemann's Legacy to High Energy Physics and Cosmology* (Springer, New York, 2011).
 - [4] P. Badyopadhyay, *Geometry, Topology and Quantum Field Theory* (Springer, Dordrecht, 2003).
 - [5] D. R. Nelson, *Defects and Geometry in Condensed Matter Physics* (Cambridge University Press, Cambridge, 2002).
 - [6] R. D. Kamien, The geometry of soft materials: A primer, *Rev. Mod. Phys.* **74**, 953 (2011).
 - [7] R. Kallosh and A. Linde, Escher in the sky, *C. R. Phys.* **16**, 914 (2015).
 - [8] H. Spohn, The Lorentz process converges to a random flight process, *Commun. Math. Phys.* **60**, 277 (1978).
 - [9] E. Orsingher, C. Ricciuti, and F. Sisti, Motion among random obstacles on a hyperbolic space, *J. Stat. Phys.* **162**, 869 (2016).
 - [10] W. Kung, *Geometry and Phase Transitions in Colloids and Polymers* (World Scientific, Singapore, 2009).
 - [11] G. Ruppeiner, A. Sahay, T. Sarkar, and G. Sengupta, Thermodynamic geometry, phase transitions, and the Widom line, *Phys. Rev. E* **86**, 052103 (2012).
 - [12] R. Rietman, B. Nienhuis, and J. Oitmaa, The Ising model on hyperlattices, *J. Phys. A* **25**, 6577 (1992).
 - [13] C. C. Wu, Ising models on hyperbolic graphs, *J. Stat. Phys.* **85**, 251 (1996).

- [14] D. Gandolfo, J. Ruiz, and S. Shlosman, A manifold of pure Gibbs states of the Ising model on the Lobachevsky plane, *Commun. Math. Phys.* **334**, 313 (2015).
- [15] R. Krcmar, T. Iharagi, A. Gendiar, and T. Nishino, Tricritical point of the $J_1 - J_2$ Ising model on a hyperbolic lattice, *Phys. Rev. E* **78**, 061119 (2008).
- [16] R. Krcmar, A. Gendiar, K. Ueda, and T. Nishino, Ising model on a hyperbolic lattice studied by the corner transfer matrix renormalization group method, *J. Phys. A* **41**, 125001 (2008).
- [17] H. Shima and Y. Sakaniwa, Geometric effects on critical behaviours of the Ising model, *J. Phys. A* **39**, 4921 (2006).
- [18] H. Gu and R. M. Ziff, Crossing on hyperbolic lattices, *Phys. Rev. E* **85**, 051141 (2012).
- [19] S. K. Baek, P. Minnhagen, and B. J. Kim, Surface and bulk criticality in midpoint percolation, *Phys. Rev. E* **81**, 041108 (2010).
- [20] S. K. Baek, P. Minnhagen, and B. J. Kim, Percolation on hyperbolic lattices, *Phys. Rev. E* **79**, 011124 (2009).
- [21] I. Benjamini and O. Schramm, Percolation in the hyperbolic plane, *J. Am. Math. Soc.* **14**, 487 (2000).
- [22] G. Tarjus, S. A. Kivelson, Z. Nussinov, and P. Viot, The frustration-based approach to supercooled liquids and the glass transition: A review and critical assessment, *J. Phys.: Condens. Matter* **17**, R1143 (2005).
- [23] C. D. Modes and R. D. Kamien, Geometrical frustration in two dimensions: Idealizations and realizations of a hard-disk fluid in negative curvature, *Phys. Rev. E* **77**, 041125 (2008).
- [24] H. S. M. Coxeter, *Regular Polytopes*, 3rd ed. (Dover, New York, 1973).
- [25] J. Raffield, H. L. Richards, J. Molchanoff, and P. A. Rikvold, Phase separation on a hyperbolic lattice, *Phys. Proc.* **53**, 82 (2014).
- [26] J. Anderson, *Hyperbolic Geometry*, 2nd ed. (Springer, London, 2008).
- [27] J. Chalupa, P. L. Leath, and G. R. Reich, Bootstrap percolation on a Bethe lattice, *J. Phys. C* **12**, L31 (1979).
- [28] J. M. Schwarz, A. J. Liu, and L. Q. Chayes, The onset of jamming as the sudden emergence of an infinite k -core cluster, *Europhys. Lett.* **73**, 560 (2006).
- [29] M. Jeng and J. M. Schwarz, Force-balance percolation, *Phys. Rev. E* **81**, 011134 (2010).
- [30] S. Alexander, Amorphous solids: Their structure, lattice dynamics, and elasticity, *Phys. Rep.* **296**, 65 (1998).
- [31] C. S. O'Hern and L. E. Silbert, Jamming at zero temperature and zero applied stress: The epitome of disorder, *Phys. Rev. E* **68**, 011306 (2003).
- [32] M. C. Medeiros and C. M. Chaves, *Physica A* **234**, 604 (1997).
- [33] A. C. D. van Enter, Proof of Straley's argument for bootstrap percolation *J. Stat. Phys.* **48**, 943 (1987).
- [34] C. S. O'Hern, S. A. Langer, A. J. Liu, and S. R. Nagel, Random Packings of Frictionless Particles, *Phys. Rev. Lett.* **88**, 075507 (2002).
- [35] F. Sausset, C. Toninelli, G. Biroli, and G. Tarjus, Bootstrap percolation and kinetically constrained models on hyperbolic lattices, *J. Stat. Phys.* **138**, 411 (2010).
- [36] D. Dunham, Hyperbolic symmetry, *Comput. Math. Appl.* **12**, 139 (1986).
- [37] F. Sausset and G. Tarjus, Periodic boundary conditions on the pseudosphere, *J. Phys. A* **40**, 12873 (2007).
- [38] S. S. Manna, Abelian cascade dynamics in bootstrap percolation, *Physica A* **261**, 351 (1998).
- [39] J. Czajkowski, Clusters in middle-phase percolation on hyperbolic plane, *Banach Center Publ.* **96**, 99 (2012).
- [40] J. F. Lee and S. K. Baek, Bounds of percolation thresholds on hyperbolic lattices, *Phys. Rev. E* **86**, 062105 (2012).
- [41] J. L. Cardy, Critical percolation in finite geometries, *J. Phys. A* **25**, L201 (1992).
- [42] D. Stauffer and A. Aharony, *Introduction to Percolation Theory*, 2nd ed. (Taylor and Francis, New York, 1992).
- [43] S. K. Baek, Upper transition point for percolation on the enhanced binary tree: A sharpened lower bound, *Phys. Rev. E* **85**, 051128 (2012).
- [44] A. B. Harris, Field-theoretic approach to biconnectedness in percolating systems, *Phys. Rev. B* **28**, 2614 (1983).
- [45] A. B. Harris and J. M. Schwarz, $1/d$ expansion for k -core percolation, *Phys. Rev. E* **72**, 046123 (2005).